Predator-prey model for simulating the genetic carcinogenicity of aggressive toxicant-related cancer

Journal:	*Journal of Applied Toxicology*
Manuscript ID	JAT-25-0187
Wiley - Manuscript type:	Research Article
Date Submitted by the Author:	18-Mar-2025
Complete List of Authors:	Fernández-González, Mauricio; Universidad del Desarrollo Facultad de Medicina Armisen, Ricardo; Universidad del Desarrollo Facultad de Medicina Fernández, Mario I.; Universidad del Desarrollo Facultad de Medicina; Clinica Alemana de Santiago SA
Keywords:	Cancer, aggressiveness, growth, stress response, toxicity, cadmium, copper, carboplatin

Predator-prey model for simulating the genetic carcinogenicity of aggressive toxicant-related cancer

Short title: Predator-prey model for simulating carcinogenicity of toxicant-driven cancer

Mauricio Fernández-González [a], Ricardo Armisen [a], Mario I. Fernández [a,b*]

[a] *Centro de Genética y Genómica, Instituto de Ciencias e Innovación en Medicina, Facultad de Medicina Clínica Alemana, Universidad del Desarrollo, Santiago, Chile.*

[b] *Departamento de urología, Clinica Alemana, Universidad del Desarrollo, Santiago, Chile.*

**** Corresponding author*** mariofernandez@udd.cl

Abstract. The mechanism of how toxicant exposure leads to aggressive tumors remains unresolved. A genetic-based hypothesis predicts that under stress, the transcription of growth-related genes will be inhibited by the activation of mitogenic pathways, redirecting energy toward stress response and increasing survival. This hypothesis fails to explain why epidemiological data suggest that growth and stress response are activated, as patients exposed to toxicants exhibit more aggressive growth than non-exposed individuals. This co-occurrence requires increased energy availability to prevent the activation of mitogenic pathways, as seen in the Warburg effect. We hypothesize that if pollutant effects cease might drives aggressive cancer, as excess energy no longer used for stress response can fuel rapid growth. We model this allocation between growth and stress response as a trophic competition using Lotka-Volterra equations and using as input RNA-Seq data from growth- and stress-related genes obtained from cancer cells exposed to copper, cadmium, and carboplatin. Our findings suggest that the energy allocation to growth and its rate of allocation is higher in exposed than non-exposed tumors and results in overgrowth in unexposed cells. This study helps to understand how certain scenarios, such as partial or total cessation of exposure, in toxicant-related cancer can drive cancer aggressiveness.

Short Abstract. The link between toxicant exposure and aggressive tumors remains unclear. While stress response inhibits growth-related genes, epidemiological data show both are activated in exposed patients. We propose that exposure cessation drives tumor aggressiveness by redirecting the energy no longer used to stress response to growth. Using Lotka-Volterra modeling with RNA-Seq data from cancer cells exposed to copper, cadmium, and carboplatin, we show that the rate and total energy allocated to growth are higher in exposed tumors

Introduction

Epidemiological studies estimate that environmental factors contribute to approximately 80% of cancers (Lagoa et al. 2022). Toxicant exposure can transform normal cells into malignant ones by generating reactive oxygen species, inhibiting DNA repair mechanisms (Andrew et al. 2006), and interfering with signal transduction, cell proliferation, and programmed cell death (Ai et al. 2007). Additionally, toxicants increase DNA reactivity in cells, disrupt mitotic spindle interactions, cause cytotoxicity, and trigger tissue regeneration (Cohen et al. 2006). These effects contribute to cancer-specific phenotypes, including sustained proliferative signaling, resistance to cell death, evasion of growth suppression, replicative immortality, inflammation, metabolic dysregulation, genomic instability, angiogenesis induction, and invasion leading to metastasis (Lagoa et al. 2022).

An important characteristic of toxicant-related cancer is its potential to exhibit more aggressive growth than tumors in unexposed individuals (Moore et al. 2002; Fernández et al. 2020; Pal et al. 2020; Ghosh et al. 2021). However, the mechanisms by which toxicant exposure leads to highly

aggressive tumors remain unclear. Genetic-based hypotheses further complicate this scenario, suggesting that the activation of mitogenic pathways may inhibit the transcription of growth-related genes to redirect energy toward survival. Emerging evidence indicates that cells finely regulate the balance between stress-related and growth-related gene expression, two opposing programs controlled by distinct regulatory mechanisms. This switching mechanism is composed by the existence of two main signaling pathways coupled to respond to environmental conditions: (i) TOR, a pathway that promotes growth, and (ii) the mitogenic pathway MAPK-related protein kinase that increases stress resistance (Lopez-Maury, Marguerat and Bähler 2008). Under stressful conditions, MAPK inhibits the TOR pathway, leading to a decrease in growth, while under a favorable environment the TOR pathway inhibits MAPK related pathways, thus enhancing growth (Lopez-Maury, Marguerat and Bähler 2008). This mechanism can be seen as a strategy to optimize energy allocation, balancing growth and stress responses to adapt efficiently to stressful conditions (Lopez-Maury, Marguerat, and Bähler 2008; Fernández 2022). It enables cells to develop stress resistance under persistent and/or chronic environmental stress. Although the mTOR/MAPK negative feedback mechanism has been described as a regulator of growth and stress responses, it fails to explain why epidemiological data show that tumors in exposed patients exhibit more aggressive growth than those in non-exposed individuals (Fernández et al. 2012; Ruffino et al. 2022). which suggests that both biological functions are co-activated, enabling cancer cells to grow while resisting toxicant exposure.

The co-activation of growth and stress responses may push cells into a constrained energetic state due to excessive consumption required to sustain both biological functions. This overconsumption can lead to a metabolic condition resembling starvation, in which tumor cells exploit non-conventional metabolic pathways to obtain additional energy. This co-activation under starvation may be possible due to phenomena like the Warburg effect (Liberti and Locasale 2016), which enables rapid energy production through glycolysis, providing sufficient energy to support tumor growth and other biological processes, such as the stress response, while preventing mitogenic pathways from inhibiting cell growth.

From an ecological perspective, the allocation of energy between growth and stress response in a constrained state mirrors a competitive scenario similar to the trophic competition between two species for the same resource. As extensively studied, a critical phase in this competition arises when one species is eliminated, allowing the surviving species to exploit all newly available resources, which in turn accelerates its population growth. Taking this example of trophic competition and considering the competitive interplay between the co-activation of growth and stress response, we hypothesize that the activation of these three components—growth, energy, and stress response—is key to the development of aggressive cancer if pollutant exposure ceases. In this scenario, aggressive growth could be fueled by the excess energy that cells no longer need for stress response. We use the Lotka-Volterra (LV) competition equations—mathematical models traditionally applied in ecology to study resource competition between two species—to mathematically model energy allocation dynamics between growth and stress response as a trophic competition problem. This approach allows us to examine the effect of stress response extinction on energy allocation to tumor growth. To parameterize the model, we use RNA-Seq data from growth- and stress-related genes obtained from cancer cells exposed to copper, cadmium, and carboplatin. This ecological framework allowed us to study not only the dynamics of energy allocation between both biological processes but also to gain insights into the etiology and

aggressiveness of cancers exposed to environmental toxicants, including the resistance of certain tumors to chemotherapy—a phenomenon that remains poorly understood.

Materials and methods

We modeled the competition for energy between growth and stress response using publicly available RNA-Seq data from three cancer types related to toxicant exposure. We identified the two biological functions by searching for the IDs of differentially expressed genes in GeneCards (Stelzer et al. 2016) and by searching for gene IDs linked with the terms "cancer" and "tumor" in PubMed. We analyzed transcriptional data from renal cell carcinoma cells exposed to copper (Bischoff et al. 2024) and breast cancer cells exposed to cadmium (Lubovac-Pilav et al. 2013). Furthermore, to assess the impact of chemotherapies on aggressive tumor growth, we included an analysis of carboplatin exposure in endometrial cancer cells (Hellweg et al. 2018). See the supplementary materials for details on the RNA-Seq data filtering methods.

To model the competition between growth and stress response, we use the Lotka-Volterra (LV) model, a system of differential equations historically employed in ecology to describe interactions between species. We consider Equation 1 as a special case of interaction, where the competition is for the same resource, including trophic interactions. We will model this competition by assessing the impact of reducing one biological function (the extinction of one species) on the other, assuming that WE is activated to fuel both growth and stress response, and that its activation remains available after the extinction of the stress response.

This equation system is used to model the dynamic in time t of the growth of populations that exploit the same resource. In this LV equations r_i is the maximum prey per capita growth rate for the species i and x_i is the density of populations for the species i, k_i is the carrying capacity for the species i (maximum individuals that environment support) and a_{ij} is the effect of specie i on specie j.

$$dx_1/dt = r_1 x_1 (1 - (x_1 - a_{12} x_2) / k_1)$$
$$dx_2/dt = r_2 x_2 (1 - (x_2 - a_{21} x_1) / k_2) \qquad eq.\ 1$$

We used LV competitive equations model to exemplify the competition for energy between the growth and stress-response. In equation 1, x_1 x_2 are the energy allocated to biological function 1 (F1) and biological function 2 (F2), r_1 r_2 are the rate of energy allocation to F1 and F2 correspondingly, and k_1 k_2 are the carrying capacity for both functions. a_{12} and a_{21} are the effect of F1 on F2, and the effect of F2 in F1 correspondingly. For each data set, the values of x_1 and x_2 (energy allocated to F1 and F2) where obtained from the multiplication between the fold-change value and the by the total cost in ATP form of synthesize all the amino acids derived from the primary transcript according to Craig and Weber (1998), that allows to obtain the pondered cost of synthesize the amino acids derived from primary transcripts. We obtain the values of k_1 k_2 from the estimation of total production of ATP from events of Krebs cycle and glycolysis per day, using equation 2. All calculation were made using shell scripting under Linux OS and are available as supplementary materials.

$$k = N_m * M_{ck} * 32(ATP) * 0.001666563 * 60\ (min) * 60\ (hour) * 24\ (day) \qquad eq.\ 2$$

In equation 2 N_m is the number of mitochondria in a eucaryotic cell, M_{ck} is the number of Kreb cycle per mitochondria, *32(ATP)* is the final ATP produced by each Kreb cycle. *0.001666563* allows to express the energy obtained in seconds. *60 (min)* is the conversion of second to minutes and *60 (hour)* is the conversion of minutes to hours, and *24 (day)* is the conversion of hours to one day. Because there is no clarity about the number of events of Kreb Cycle and glycolysis in a cell, but it is known that there is thousand KC in a cell occurring at the same time, we defined as 1000 the number of events of Kreb cycle and glycolysis, per mitochondria and cells correspondingly. We use the same value for k_1 k_2 considering that both functions can exploit the same source of energy. We set the same value (-0.5) of the effect of F1 and F2 and vice versa (a_{12} and a_{21}). Finally, we set the value of r_1 r_2 as the standardized stoichiometric exponent for metabolic rates (Brown et al. 2004) equal to 0.75 for r_1 and –0.75 for r_2.

To test the dynamic of energy allocation between growth and stress-response assumes that WE remain active after one biological function decay, in this scenario and to test the effect of the free energy available from WE in the energetic dynamic of biological functions, we set r_1 as positive value and r_2 as negative value to model the decay of the F2 while F1 is still active. a_{12} and a_{21} also take negative values, because they represent the fight between biological functions for energy. The parameters r_2 and a_{21}, r_2 that takes a negative value because the F2 is decreasing, therefore the negative effect on F1 due to the negative value of a_{21} decreases. This decrease in negative effect is the allocation of extra energy from F2 to F1 that can be obtained from WE. Finally, to compare the energy allocation to biological functions of exposed cells with the allocation of unexposed cells, the allocation to growth on non-exposed tumors was modeled using equation 3 that does not involve interaction and only includes the analysis of allocation to growth related genes, the parameters were set to: r_3 =0.75; x_3 is the energy used to the biological function from RNASeq data in ATP form; k_3 carrying capacity in ATP form calculated according to *eq 2*.

All the calculations were made using R languaje, the differential equation systems were solved using the deSolve R package (Soetaert, Petzoldt and Setzer 2010). All scripts and model parameter values are available as supplementary materials.

Results

Our model shows that a decrease in pollutant exposure leads to increased energy allocation for the transcription of growth-related genes, which is inversely correlated with a reduction in energy allocated for the transcription of stress-related genes (Figure 1 A-C). This energy allocation to growth-related genes is higher in exposed cells compared to non-exposed ones across all tested toxicants. Our results also show that the rate of allocation to tumor growth is increased, suggesting that this shift in energy allocation could potentially have harmful short-term effects.

Discussion

Our model shows that when the effect of toxicants ceases, cancer cells allocate more energy to growth, resulting in an increased rate of energy allocation to this process. These findings suggest that toxicant exposure may lead to a short-term boost in tumor growth, driven by an additional energy input. This increase in energy, likely originating from an alternative metabolic pathway such as the Warburg effect (WE), is implicit in the model because the incorporation of both growth and stress response into the equations requires extra energy to prevent the activation of mitogenic

pathways, which would otherwise inhibit growth and redirect energy to stress response. We predict that once the toxicant effect stops, the mTOR pathway becomes more activated while the mitogenic pathway is suppressed, allowing for a high energy allocation to growth and fueling aggressive tumorigenesis.

The increase in the rate of resource allocation may result from the recruitment of additional energy sources. In this case, cell growth is supported by energy derived from the deactivation of stress-related functions. It is known that the size-specific metabolic rate generally approaches 0.75 (Brown et al. 2004), indicating that metabolism is lower than what would be predicted based on body size (which should be close to 1). Any increase above 0.75 suggests that cells are supplemented by an additional energy input, enabling them to elevate their metabolic rate. We hypothesize that the observed increase in the rate of energy allocation to growth might reflect an underlying increase in the size-specific metabolic rate, driven by an extra energy input, such as that obtained through the activation of the Warburg effect (WE). This increased allocation rate and the utilization of energy is critical, as it contributes to cancer aggressiveness by shortening the energy allocation period and promoting rapid tumor expansion. In ecological terms, the rise in energy availability can be interpreted as an increase in carrying capacity (k), which represents the maximum population size the environment can support. In this context, WE acts as an alternative foraging strategy that ultimately fuels the higher growth characteristic of aggressive tumors in exposed conditions.

A key factor in the increase of energy production due to the activation of alternative metabolic mechanisms is the emergence of energy-stressed states that create a cellular demand for energy. This energy deficit can arise not only from the demands of growth and stress response but also from the direct harmful effects of toxicants on the energy production machinery, leading to a reduction in available energy. Both phenomena trigger the activation of alternative energy acquisition pathways, ultimately promoting growth. Below, we examine the mechanistic impact of toxicant exposure on growth promotion, energy production machinery, and stress response, which is one of the main assumptions of the model.

THE ROLE OF TOXICANTS IN UNCONTROLLED CELL GROWTH

Exposure to heavy metals can significantly impact cellular growth and proliferation, playing a critical role in cancer development and progression. It interferes with key molecular pathways that regulate the cell cycle, apoptosis, and DNA repair, while also supporting angiogenesis and metastasis. Specifically, copper is an essential micronutrient required for cell proliferation and spreading (Lopez, Ramchandani, and Vahdat 2019), and is crucial for tumor growth, angiogenesis, and metastasis. Cancer cells exhibit increased copper dependency, and cancer patients show elevated serum and tumor copper levels compared to healthy controls (Gupte and Mumper 2009). This toxicant activates mitogen-activated protein kinases, such as RAS-RAF-MEK-ERK, which are involved in cell proliferation and facilitate angiogenesis through vascular endothelial growth factor and other pro-angiogenic factors (da Silva et al. 2022; Harris 2004). Copper also supports metastasis and invasion through copper-dependent enzymes and other proteins, such as LOX, SPARC, and NF-κB (Li 2020).

Cadmium may promote tumor growth by suppressing tumor suppressor genes and inhibiting pathways involved in DNA repair following mutations (Song et al. 2015). This toxicant contributes to cancer progression by mimicking steroid hormones, such as estrogen, stimulating cell

proliferation and inhibiting apoptosis pathways (Byrne et al. 2009; Joseph 2009). Additionally, cadmium inhibits DNA repair mechanisms and induces oxidative stress, leading to genomic instability (Song et al. 2015; Luevano and Damodaran 2014). In breast cancer, cadmium activates estrogen receptor alpha (ERα), contributing to cell proliferation (Stoica et al. 2000). It also increases cellular invasiveness and higher histological grade tumors by altering the expression and activation of the KRAS proto-oncogene, as well as transcription factors like TWIST1 and NUPR1 (Wu et al. 2022), and increases telomerase activity (Martínez-Campa et al. 2008). Furthermore, cadmium exposure promotes malignant progression by enhancing migratory and invasive capabilities through the upregulation of the TGIF/MMP2 signaling axis (TG-interacting factor/matrix metalloproteinase) (Wang et al. 2019). It also facilitates cell cycle progression in a triple-negative cell line by increasing the expression of cyclins A, B, and E, as well as CDKs 1 and 2 (Wei et al. 2015).

Other toxicants, such as arsenic, can also influence cell proliferation through Dimethylarsinic acid (DMA), a byproduct of arsenic processing that promotes cell proliferation by decreasing apoptosis, inhibiting terminal differentiation, and increasing cellular birth rates (Cohen 1998; Cohen et al. 2007). DMA can also cause regenerative hyperplasia, a phenomenon involved in cellular proliferation that contributes to cancer growth (Dodmane et al. 2013).

Despite differences in their mechanisms of action, the effects of these stressors converge in promoting cellular proliferation and survival by hijacking normal regulatory processes. These alterations not only sustain uncontrolled growth but also facilitate metastasis and therapy resistance, underscoring the need for targeted interventions to mitigate their oncogenic potential.

MECHANISMS OF ENERGY DISRUPTION BY COPPER, AND CADMIUM

The coactivation of growth and stress response, along with the resulting uncontrolled cell growth, demands additional energy input. This demand is amplified not only by the increased energy required to sustain both functions but also by the harmful effects of toxicants on the energy production machinery, could lead to an energy-stressed state and to request additional energy to maintain its functions. Copper and cadmium disrupt cellular energy homeostasis through several mechanisms, some common to all three toxicants, primarily targeting mitochondrial function. These metals share pathways that impair energy production, promote mitochondrial dysfunction, and contribute to cellular stress, ultimately favoring pathological outcomes. It is important to note that, to promote growth, the harmful impact on mitochondria must be partial, as this prevents apoptosis and allows the cell to survive. Next, we examine how toxicants impact the cellular energy production machinery.

Mitochondrial dysfunction

Copper and cadmium both compromise mitochondrial integrity and functionality. They disrupt the electron transport chain (ETC) by inhibiting key enzymatic complexes, such as Complexes I, II, III, and IV, leading to decreased oxidative phosphorylation efficiency and ATP synthesis (Belyaeva et al. 2004; Nadanaciva et al. 2007; Branca et al. 2020). Cadmium inhibits NADH-coenzyme Q reductase downstream, reducing respiratory activity (Ciapaite et al. 2009; Jomova et al. 2011). Copper, on the other hand, reduces mitochondrial membrane potential and alters ATP/ADP ratios through interactions with multiple ETC complexes (Hosseini et al. 2014). Other toxicants, such as arsenic, also promote glycolysis by generating reactive oxygen species, which

activate NF-κB signaling pathways (Yin et al. 2024b). In addition, arsenic can interfere with pyruvate dehydrogenase and mimic phosphate groups, leading to the production of non-functional ADP-arsenate.

ATP depletion

Copper and cadmium significantly reduce cellular ATP levels by impairing the mitochondrial respiratory chain and uncoupling oxidative phosphorylation. For instance, cadmium stimulates proton (H^+) influx, dissipating energy as heat rather than synthesizing ATP (Koike et al. 1991), while copper inhibits ATP synthesis by interacting with ATP synthase and disrupting the activity of respiratory complexes (Hosseini et al. 2014).

Structural damage to mitochondria

Mitochondrial membrane integrity is a common target of these metals, resulting in swelling, increased permeability, and the release of cytochrome c. These changes promote apoptosis and necrosis by activating caspase-dependent pathways and opening mitochondrial permeability transition pores (Belyaeva et al. 2004; Gobe and Crane 2010; Seth et al. 2004).

TOXICANTS AND WARBURG EFFECT

As has been seen, cadmium and copper can disrupt normal ATP production, causing an energy-constrained state that supports the energy requirements of tumor growth and the stress response, potentially triggering the activation of the Warburg effect (WE). Specifically, cadmium has been shown to elevate the basal glycolytic rate in a time-dependent manner by increasing glucose uptake, lactate release, ATP production, and the protein levels of key glycolytic enzymes in A549 and HELF cells (Wang et al. 2020). Differential expression of genes related to the Warburg effect, including HIF1A, GLUT1, and PKM, has been observed in cadmium-exposed tumor tissues (Tarhonska et al. 2023). The activation of HIF1A, a crucial regulator of the Warburg effect, results in the upregulation of glucose transporters and glycolytic enzymes, thereby enhancing glycolytic flux and promoting tumorigenesis (Masoud and Li 2015). Cadmium exposure was positively correlated with the expression of GLUT1 and PKM, key components of the glycolytic pathway (Woo et al. 2015). The overexpression of GLUT1 was associated with poor prognosis in breast cancer, further emphasizing the role of glycolysis in cadmium-induced cancer progression (Deng et al. 2018). This reprogramming, driven by the upregulation of key glycolytic enzymes such as GLUT1, HK2, and PKM2, is central to WE and plays a significant role in the carcinogenic potential of these pollutants.

Copper exposure can lead to mitochondrial disruption, especially through copper-depleting nanoparticles (CDNs). In triple-negative breast cancer (TNBC) cells treated with CDNs, mitochondrial oxidative phosphorylation is inhibited, causing a metabolic shift toward glycolysis and a reduction in ATP production (Cui et al. 2021). This metabolic reprogramming, similar to the effects observed with arsenic and cadmium exposure, involves the upregulation of glycolytic enzymes and the suppression of oxidative phosphorylation. These changes suggest that these environmental contaminants promote the Warburg effect through shared molecular mechanisms

The activation of WE has also been extensively studied in cells exposed to arsenic. Arsenic-treated lung epithelial cells show increased glucose uptake and lactic acid production (He et al. 2019), along with the upregulation of glycolysis-related genes such as hexokinase 2 (HK2),

phosphoglycerate kinase 2 (PGK2), and fructose-1,6-diphosphatase (FBP2) (Bi et al. 2020), all of which promote and are associated with the activation of glycolysis. Moreover, arsenic exposure activates key glycolytic enzymes, including pyruvate kinase M2 (PKM2), a central regulator of cancer cell metabolism and proliferation (Wang et al. 2020). The arsenic-induced upregulation of glucose transporter 1 (GLUT1), LDHA, and PKM2 has been linked to increased cell viability and proliferation, further emphasizing the role of the Warburg effect in arsenic-driven carcinogenesis (Yin et al. 2024a). Additionally, the generation of reactive oxygen species (ROS) promotes glycolysis and cell growth by activating signaling pathways such as NF-κB (Yin et al. 2024b).

CARBOPLATIN AND CHEMORESISTANCE

Carboplatin is a chemotherapeutic agent used in the treatment of various tumor types, including ovarian, head and neck, and small cell lung cancer (Fuertes, Alonso, and Perez 2003). The primary target of carboplatin is DNA, where it inhibits replication and transcription, ultimately inducing apoptosis (Brabec and Kasparkova 2005). Despite its success in treating many cancer cases, a subset of patients develops chemoresistance to this drug, a phenomenon that remains poorly understood. The DNA repair pathway plays a crucial role in cellular resistance to carboplatin, with the activation of nucleotide excision repair (NER) or mismatch repair (MMR) pathways, along with cytoplasmic stress response mechanisms, being well-established contributors to this resistance. Recent studies have also identified metal transporters, including copper transporters such as CTR1, ATP7A, and ATP7B, as additional mechanisms driving carboplatin resistance, as they participate in the efflux of the drug (Cui et al. 1999; Katano et al. 2003; Samimi et al. 2004).

At the energetic level, cisplatin can affect mitochondrial function by inducing the formation of reactive oxygen species (ROS), which alters the mitochondrial membrane potential and damages respiratory chain transporters, ultimately triggering the apoptotic process (Kleih et al. 2019). However, to fully understand the effect of ROS on mitochondria, it is crucial to consider the intermediate states that may precede ROS-mediated apoptosis. This suggests that mitochondria can be affected by carboplatin or other toxicants to a degree that does not induce apoptosis. For example, cisplatin induces cytotoxicity in ovarian cancer cells, but when ROS levels do not reach cytotoxic thresholds, cancer cells may develop chemoresistance (Kleih et al. 2019).

The clinical significance of the various resistance mechanisms examined for the toxicants in this study remains unclear. However, a key characteristic contributing to chemoresistance and tumor aggressiveness in toxicant-exposed cells is not only their ability to survive chemotherapy and continue growing, but also the ability of cells lacking sufficient resistance to temporarily downregulate proliferation and enter a quiescent state until treatment cessation (Stewart 2007). This cellular shutdown aligns with our findings on the competition for energy between growth and stress response, showing an increase in growth when the effects of toxicants decrease.

Understanding the mechanisms of energy disruption and cellular dysregulation induced by toxicant exposure provides valuable insights for developing therapeutic strategies to mitigate oncogenic effects and improve outcomes in toxicant-related cancers, particularly in chemotherapy-resistant tumors, where the cessation of toxicants may drive recurrent and aggressive tumor growth.

Conclusion

Our findings suggest that aggressive cancer development is driven by the simultaneous activation of stress response and growth under limited energy availability, which is promoted by toxicant-

induced damage to energy production. This co-occurrence activates the Warburg effect (WE), resulting in an increased energy budget that, as the toxicant's effect diminishes, can be fully redirected to growth, thereby enhancing tumor aggressiveness. This study helps to understand how certain scenarios, such as partial or total cessation of exposure, in toxicant-related cancer can drive cancer aggressiveness and may be particularly relevant in chemotherapy-resistant tumors, where the cessation of toxicant exposure— as during the inter-cycle of therapy —can drive recurrent and aggressive tumor growth.

Funding details
This work was supported by the Agencia Nacional de Investigación y Desarrollo under grant Proyecto Anillo ACT210079, awarded to Mario Fernández and Ricardo Armisen.

Disclosure statement
The authors report there are no competing interests to declare.

Data availability statement.
The data used are available at: doi:10.1158/2159-8290.CD-24-0187; doi:10.1371/journal.pone.0084646; doi:10.1007/s12672-018-0337-6

Ethics Approval
As this is mathematical modeling based on previously published data from cell lines, ethical committee approval was not required

Supplementary materials
Supplementary materials are available and include R and shell scripting scripts.

Conflict of interest
There are no conflicts of interest to declare.

AI usage disclosure
We used ChatGPT-4 to generate alternative phrasing for some manuscript sentences, aiming to enhance the clarity of the information presented.

Acknowledgment
We would like to thank Javier Gonzalez Barrientos for his help in answering questions about the effects of toxicants on cells.

Reference list

Ai, Z., Lu, W., Ton, S., Liu, H., Sou, T., Shen, Z., and Qin, X. (2007). Arsenic trioxide-mediated growth inhibition in gallbladder carcinoma cells via down-regulation of Cyclin D1 transcription mediated by Sp1 transcription factor. *Biochem. Biophys. Res. Commun.* 360(3), 684-689. https://doi.org/10.1016/j.bbrc.2007.06.123

Andrew, A. S., Burgess, J. L., Meza, M. M., Demidenko, E., Waugh, M. G., Hamilton, J. W., and Karagas, M. R. (2006). Arsenic exposure is associated with decreased DNA repair in vitro and in individuals exposed to drinking water arsenic. *Environ. Health Perspect.* 114(8), 1193-1198. https://doi.org/10.1289/ehp.9008

Belyaeva, E., Glazunov, V., and Korotkov, S. (2004). Cd2+-promoted mitochondrial permeability transition: a comparison with other heavy metals. *Acta Biochim. Pol*. 51(2), 545-551.

Bi, Z., Zhang, Q., Fu, Y., Wadgaonkar, P., Zhang, W., Almutairy, B., ... and Chen, F. (2020). Nrf2 and HIF1α converge to arsenic-induced metabolic reprogramming and the formation of the cancer stem-like cells. *Theranostics,* 10(9), 4134. doi:10.7150/thno.42903

Bischoff, M. E., Shamsaei, B., Yang, J., Secic, D., Vemuri, B., Reisz, J. A., ... and Czyzyk-Krzeska, M. F. (2024). Copper drives remodeling of metabolic state and progression of clear cell renal cell carcinoma. *Cancer Discov*. doi:10.1158/2159-8290.CD-24-0187

Brabec, V., and Kasparkova, J. (2005). Modifications of DNA by platinum complexes: relation to resistance of tumors to platinum antitumor drugs. *Drug Resist. Updat*. 8(3), 131-146. doi:10.1016/j.drup.2005.04.006

Branca, J. J. V., Pacini, A., Gulisano, M., Taddei, N., Fiorillo, C., and Becatti, M. (2020). Cadmium-induced cytotoxicity: effects on mitochondrial electron transport chain. Front. Cell Dev. Biol. 8, 604377. doi: 10.3389/fcell.2020.604377

Brown, J. H., Gillooly, J. F., Allen, A. P., Savage, V. M., and West, G. B. (2004). Toward a metabolic theory of ecology. *Ecology.* 85(7), 1771-1789. doi: 10.1890/03-9000

Byrne, C., Divekar, S. D., Storchan, G. B., Parodi, D. A., and Martin, M. B. (2009). Cadmium—a metallohormone?. *Toxicol. Appl. Pharmacol*. 238(3), 266-271. doi:10.1016/j.taap.2009.03.025

Ciapaite, J., Nauciene, Z., Baniene, R., Wagner, M. J., Krab, K., and Mildaziene, V. (2009). Modular kinetic analysis reveals differences in Cd2+ and Cu2+ ion-induced impairment of oxidative phosphorylation in liver. The *FEBS J*. 276(13), 3656-3668. doi:10.1111/j.1742-4658.2009.07084.x

Cohen, S. M. (1998). Urinary bladder carcinogenesis. *Toxicol. Pathol*. 26(1), 121-127.

Cohen, S. M., Arnold, L. L., Eldan, M., Lewis, A. S., and Beck, B. D. (2006). Methylated arsenicals: the implications of metabolism and carcinogenicity studies in rodents to human risk assessment. *Crit. Rev. Toxicol*. 36(2), 99-133. doi:10.1080/10408440500534230

Craig, C. L., and Weber, R. S. (1998). Selection costs of amino acid substitutions in ColE1 and ColIa gene clusters harbored by Escherichia coli. *Mol. Biol. Evol*. 15(6), 774-776.

Cui, Y., König, J., Buchholz, U., Spring, H., Leier, I., and Keppler, D. (1999). Drug resistance and ATP-dependent conjugate transport mediated by the apical multidrug resistance protein, MRP2, permanently expressed in human and canine cells. *Mol Pharmacol.* 55(5), 929-937. doi:10.1016/S0026-895X(24)23190-4

Cui, L., Gouw, A. M., LaGory, E. L., Guo, S., Attarwala, N., Tang, Y., ... and Rao, J. (2021). Mitochondrial copper depletion suppresses triple-negative breast cancer in mice. Nat. Biotechnol. 39(3), 357-367. doi:10.1038/s41587-020-0707-9

da Silva, D. A., De Luca, A., Squitti, R., Rongioletti, M., Rossi, L., Machado, C. M., and Cerchiaro, G. (2022). Copper in tumors and the use of copper-based compounds in cancer treatment. *J. Inorg. Biochem*. 226, 111634. doi:10.1016/j.jinorgbio.2021.111634

Deng, Y., Zou, J., Deng, T., and Liu, J. (2018). Clinicopathological and prognostic significance of GLUT1 in breast cancer: A meta-analysis. *Medicine*, 97(48), e12961. doi:10.1097/MD.0000000000012961

Dodmane, P. R., Arnold, L. L., Pennington, K. L., Thomas, D. J., and Cohen, S. M. (2013). Effect of dietary treatment with dimethylarsinous acid (DMAIII) on the urinary bladder epithelium of arsenic (+ 3 oxidation state) methyltransferase (As3mt) knockout and C57BL/6 wild type female mice. *Toxicology*, 305, 130-135. doi:10.1016/j.tox.2013.01.015

Fernández, M. I., López, J. F., Vivaldi, B., and Coz, F. (2012). Long-term impact of arsenic in drinking water on bladder cancer health care and mortality rates 20 years after end of exposure. *J. Urol*, 187(3), 856-861. doi:10.1016/j.juro.2011.10.157

Fernández, M. I., Valdebenito, P., Delgado, I., Segebre, J., Chaparro, E., Fuentealba, D., ... and Bustamante, A. (2020). Impact of arsenic exposure on clinicopathological characteristics of bladder cancer: A comparative study between patients from an arsenic-exposed region and nonexposed reference sites. In Urologic Oncology: Seminars and Original Investigations (Vol. 38, No. 2, pp. 40-e1). Elsevier. doi:10.1016/j.urolonc.2019.09.013

Fernández, M. (2022). Rapid communication: effects of cadmium exposure on the growth-related genes of Daphnia magna. *J. Toxicol. Environ. Health A*. 85(11), 457-460. doi:10.1080/15287394.2022.2034688

Fuertes, M. A., Alonso, C., and Pérez, J. M. (2003). Biochemical modulation of cisplatin mechanisms of action: enhancement of antitumor activity and circumvention of drug resistance. *Chem. Rev.* 103(3), 645-662.

Ghosh, S., Basu, M., Banerjee, K., Chaudhury, S. P., Paul, T., Bera, D. K., ... and Ghosh, A. (2021). Arsenic level in bladder tumor of patients from an exposed population: association with progression and prognosis. Future Oncol. 17(11), 1311-1323. doi:10.2217/fon-2020-0154

Gobe, G., and Crane, D. (2010). Mitochondria, reactive oxygen species and cadmium toxicity in the kidney. *Toxicol. Lett*. 198(1), 49-55. doi:10.1016/j.toxlet.2010.04.013

Gupte, A., and Mumper, R. J. (2009). Elevated copper and oxidative stress in cancer cells as a target for cancer treatment. *Cancer Treat. Rev.* 35(1), 32-46. doi:10.1016/j.ctrv.2008.07.004

Harris, E. D. (2004). A requirement for copper in angiogenesis. *Nutr. Rev.* 62(2), 60-64. doi:10.1111/j.1753-4887.2004.tb00025.x

He, J., Liu, W., Ge, X., Wang, G. C., Desai, V., Wang, S., ... and Jiang, B. H. (2019). Arsenic-induced metabolic shift triggered by the loss of miR-199a-5p through Sp1-dependent DNA methylation. *Toxicol. Appl. Pharmacol*. 378, 114606. doi:10.1016/j.taap.2019.114606

Hellweg, R., Mooneyham, A., Chang, Z., Shetty, M., Emmings, E., Iizuka, Y., ... and Bazzaro, M. (2018). RNA sequencing of carboplatin-and paclitaxel-resistant endometrial cancer cells reveals new stratification markers and molecular targets for cancer treatment. *Horm. Cancer*. 9(5), 326-337. doi:10.1007/s12672-018-0337-6

Hosseini, M. J., Shaki, F., Ghazi-Khansari, M., and Pourahmad, J. (2014). Toxicity of copper on isolated liver mitochondria: impairment at complexes I, II, and IV leads to increased ROS production. *Cell Biochem. Biophys.* 70, 367-381. doi: 10.1007/s12013-014-9922-7

Jomova, K., Jenisova, Z., Feszterova, M., Baros, S., Liska, J., Hudecova, D., ... and Valko, M. (2011). Arsenic: toxicity, oxidative stress and human disease. *J. Appl. Toxicol.* 31(2), 95-107. doi:10.1002/jat.1649

Joseph, P. (2009). Mechanisms of cadmium carcinogenesis. *Toxicol. Appl. Pharmacol*. 238(3), 272-279. doi:10.1016/j.taap.2009.01.011

Katano, K., Safaei, R., Samimi, G., Holzer, A., Rochdi, M., and Howell, S. B. (2003). The copper export pump ATP7B modulates the cellular pharmacology of carboplatin in ovarian carcinoma cells. *Mol. Pharmacol*. 64(2), 466-473. doi:10.1124/mol.64.2.466

Kleih, M., Böpple, K., Dong, M., Gaißler, A., Heine, S., Olayioye, M. A., ... and Essmann, F. (2019). Direct impact of cisplatin on mitochondria induces ROS production that dictates cell fate of ovarian cancer cells. *Cell Death Dis*. 10(11), 851. doi:10.1038/s41419-019-2081-4

Koike, H., Shinohara, Y., and Terada, H. (1991). Why is inorganic phosphate necessary for uncoupling of oxidative phosphorylation by Cd2+ in rat liver mitochondria?. *Biochim. Biophys. Acta (BBA)-Bioenergetics.* 1060(1), 75-81. doi:10.1016/S0005-2728(05)80121-5

Lagoa, R., Marques-da-Silva, D., Diniz, M., Daglia, M., and Bishayee, A. (2022, May). Molecular mechanisms linking environmental toxicants to cancer development: Significance for protective interventions with polyphenols. In Seminars in Cancer Biology (Vol. 80, pp. 118-144). Academic Press. doi:10.1016/j.semcancer.2020.02.002

Li, Y. (2020). Copper homeostasis: Emerging target for cancer treatment. *IUBMB Life*. 72(9), 1900-1908. doi:10.1002/iub.2341

Liberti, M. V., and Locasale, J. W. (2016). The Warburg effect: how does it benefit cancer cells?. *Trends Biochem. Sci*. 41(3), 21. https://doi.org/10.1016/j.tibs.2015.12.001

López-Maury, L., Marguerat, S., and Bähler, J. (2008). Tuning gene expression to changing environments: from rapid responses to evolutionary adaptation. *Nat. Rev. Genet*. 9(8), 583-593. doi: 10.1038/nrg2398

Lopez, J., Ramchandani, D., and Vahdat, L. (2019). Copper depletion as a therapeutic strategy in cancer. *Met. Ions Life Sci.* 19(10.1515), 9783110527872-018. doi:10.1515/9783110527872-012

Lubovac-Pilav, Z., Borràs, D. M., Ponce, E., and Louie, M. C. (2013). Using expression profiling to understand the effects of chronic cadmium exposure on MCF-7 breast cancer cells. *PloS one.* 8(12), e84646. doi:10.1371/journal.pone.0084646

Luevano, J., and Damodaran, C. (2014). A review of molecular events of cadmium-induced carcinogenesis. *J. Environ. Pathol. Toxicol*. Oncol. 33(3). doi:10.1615/JEnvironPatholToxicolOncol.2014011075

Martínez-Campa, C. M., Alonso-González, C., Mediavilla, M. D., Cos, S., González, A., and Sanchez-Barcelo, E. J. (2008). Melatonin down-regulates hTERT expression induced by either natural estrogens (17β-estradiol) or metalloestrogens (cadmium) in MCF-7 human breast cancer cells. *Cancer Lett*. 268(2), 272-277. doi:10.1016/j.canlet.2008.04.001

Masoud, G. N., and Li, W. (2015). HIF-1α pathway: role, regulation and intervention for cancer therapy. *Acta Pharm. Sin. B.* 5(5), 378-389. doi:10.1016/j.apsb.2015.05.007

Moore, L. E., Smith, A. H., Eng, C., Kalman, D., DeVries, S., Bhargava, V., ... and Waldman, F. M. (2002). Arsenic-related chromosomal alterations in bladder cancer. *J. Natl. Cancer Inst*. 94(22), 1688-1696. doi:10.1093/jnci/94.22.1688

Nadanaciva, S., Bernal, A., Aggeler, R., Capaldi, R., and Will, Y. (2007). Target identification of drug induced mitochondrial toxicity using immunocapture based OXPHOS activity assays. *Toxicol. In Vitro.* 21(5), 902-911. doi:10.1016/j.tiv.2007.01.011

Pal, D. K., Agrawal, A., Ghosh, S., and Ghosh, A. (2020). Association of arsenic with recurrence of urinary bladder cancer. *Trop. Doctor*, 50(4), 325-330. doi:10.1177/0049475520930155

R Core Team (2024). R: A Language and Environment for Statistical Computing_. R Foundation for Statistical Computing, Vienna, Austria. <https://www.R-project.org/>.

Ruffino, B., Campo, G., Crutchik, D., Reyes, A., and Zanetti, M. (2022). drinking water supply in the region of Antofagasta (Chile): A Challenge between Past, Present and Future. Int. J. Environ. Res. Public Health. 19(21), 14406. doi: 10.3390/ijerph192114406

Samimi, G., Safaei, R., Katano, K., Holzer, A. K., Rochdi, M., Tomioka, M., ... and Howell, S. B. (2004). Increased expression of the copper efflux transporter ATP7A mediates resistance to cisplatin, carboplatin, and oxaliplatin in ovarian cancer cells. *Clin. Cancer Res*. 10(14), 4661-4669. doi:10.1158/1078-0432.CCR-04-0137

Seth, R., Yang, S., Choi, S., Sabean, M., and Roberts, E. A. (2004). In vitro assessment of copper-induced toxicity in the human hepatoma line, Hep G2. *Toxicol. In Vitro*. 18(4), 501-509. doi: 10.1016/j.tiv.2004.01.006

Soetaert, K. E., Petzoldt, T., and Setzer, R. W. (2010). Solving differential equations in R: package deSolve. *J. Stat. Softw*. 33(9).

Song, J. K., Luo, H., Yin, X. H., Huang, G. L., Luo, S. Y., Lin, D. R., ... and Zhu, J. G. (2015). Association between cadmium exposure and renal cancer risk: a meta-analysis of observational studies. *Sci. Rep*. 5(1), 17976. doi:10.1038/srep17976

Stelzer, G., Rosen, N., Plaschkes, I., Zimmerman, S., Twik, M., Fishilevich, S., ... and Lancet, D. (2016). The GeneCards suite: from gene data mining to disease genome sequence analyses. *Curr. Protoc. Bioinformatics*. 54(1), 1-30. doi:10.1002/cpbi.5

Stewart, D. J. (2007). Mechanisms of resistance to cisplatin and carboplatin. *Crit. Rev. Oncol. Hematol*. 63(1), 12-31. doi:10.1016/j.critrevonc.2007.02.001

Stoica, A., Katzenellenbogen, B. S., and Martin, M. B. (2000). Activation of estrogen receptor-α by the heavy metal cadmium. *Mol. Endocrinol.* 14(4), 545-553. doi:10.1210/mend.14.4.0441

Tarhonska, K., Janasik, B., Roszak, J., Kowalczyk, K., Lesicka, M., Reszka, E., ... and Jablonska, E. (2023). Environmental exposure to cadmium in breast cancer–association with the Warburg effect and sensitivity to tamoxifen. *Biomed and Pharmacother.* 161, 114435. doi:10.1016/j.biopha.2023.114435

Tsuji, J. S., Chang, E. T., Gentry, P. R., Clewell, H. J., Boffetta, P., and Cohen, S. M. (2019). Dose-response for assessing the cancer risk of inorganic arsenic in drinking water: the scientific basis for use of a threshold approach. *Crit. Rev. Toxicol*. 49(1), 36-84. doi:10.1080/10408444.2019.1573804

Wang, Y., Shi, L., Li, J., Li, L., Wang, H., and Yang, H. (2019). Long-term cadmium exposure promoted breast cancer cell migration and invasion by up-regulating TGIF. *Ecotoxicol. Environ. Saf*. 175, 110-117. doi:10.1016/j.ecoenv.2019.03.046

Wang, X., Li, Z., Gao, Z., Li, Q., Jiang, L., Geng, C., ... and Cao, J. (2020). Cadmium induces cell growth in A549 and HELF cells via autophagy-dependent glycolysis. *Toxicol. In Vitro*. 66, 104834. doi:10.1016/j.tiv.2020.104834

Wei, Z., Song, X., and Shaikh, Z. A. (2015). Cadmium promotes the proliferation of triple-negative breast cancer cells through EGFR-mediated cell cycle regulation. *Toxicol. Appl. Pharmacol*. 289(1), 98-108. doi:10.1016/j.taap.2015.09.006

Woo, Y. M., Shin, Y., Lee, E. J., Lee, S., Jeong, S. H., Kong, H. K., ... and Park, J. H. (2015). Inhibition of aerobic glycolysis represses Akt/mTOR/HIF-1α axis and restores tamoxifen sensitivity in antiestrogen-resistant breast cancer cells. *PloS One.* 10(7), e0132285. doi:10.1371/journal.pone.0132285

Wu, F., Zhang, Y., Chen, X., Wang, Y., Peng, H., Zhang, Z., ... and Wang, Q. (2022). Bioinformatics analysis of key genes and potential mechanism in cadmium-induced breast cancer progression. *Environ. Sci. Pollut. Res*. 1-10. doi:10.1007/s11356-021-16542-2

Yin, F., Zhang, X., Zhang, Z., Zhang, M., Yin, Y., Yang, Y., and Gao, Y. (2024a). ERK/PKM2 Is Mediated in the Warburg Effect and Cell Proliferation in Arsenic-Induced Human L-02 Hepatocytes. *Biol. Trace Elem. Res*. 202(2), 493-503. doi:10.1007/s12011-023-03706-z

Yin, F., Zhang, Y., Zhang, X., Zhang, M., Zhang, Z., Yin, Y., ... and Gao, Y. (2024b). The ROS/NF-κB/HK2 axis is involved in the arsenic-induced Warburg effect in human L-02 hepatocytes. Int. J. Environ. Health Res. 34(1), 150-165. doi:10.1080/09603123.2022.2134559

Figures

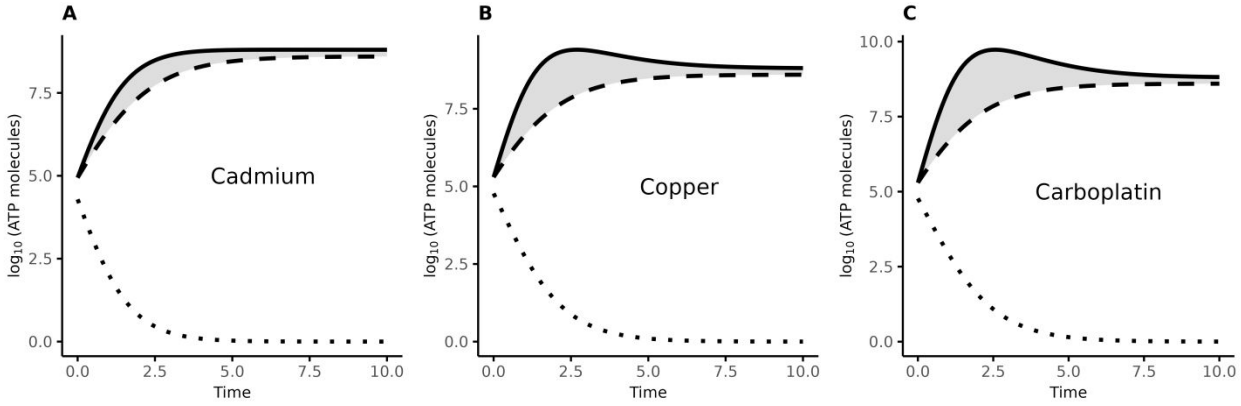

Figure legends

Figure 1. Energy allocation in tumors with and without pollutant etiology using Lotka-Volterra competitive equation. Energy competition between stress response and growth in cell lines exposed to A) Cadmium. B) Copper. C) Carboplatin. The solid line represents the growth of toxicant-exposed cell lines, the dotted line indicates the energy expended in stress-response-related functions, and the dashed line shows the growth of non-exposed cell lines. The difference in slope between the solid and dotted lines (shaded area) represents the theoretical effect of energy allocation to the growth of cancer cell lines, plus the additional energy allocated to this function by WE.

Supplementary materials.

1. Prefiltered of RNA-Seq data

1. 1. CARBOPLATIN

```
# https://link.springer.com/article/10.1186/s40659-019-0220-0#MOESM1
# Carboplatino
carboplatino=read.csv("carbopl.csv",header = T)
head(carboplatino)
dim(carboplatino)
# Filtered by p-value
carboplatino1=carboplatino[carboplatino$pval <0.05,]
dim(carboplatino1)

#Filtered by fold-change
carboplatino2=carboplatino1[carboplatino1$FC >0.5,]
dim(carboplatino2)
carboplatino3=carboplatino2[carboplatino2$FC >1.5,]
dim(carboplatino3)
```

1.2 COPPER

```
#https://aacrjournals.org/cancerdiscovery/article/doi/10.1158/2159-8290.CD-24-0187/749588
cd=read.csv("copper.csv")

# Filtered by padj
head1=cd[cd$padj<0.05,]
dim(head1)
head2=head1[head1$pval<0.05,]
dim(head2)
#Filtered by fold-change
head3=head2[head2$foldChange>1,]
dim(head3)
head4=head3[head3$foldChange>0.5,]
dim(head4)
```

1. 3 CADMIUM

```
# https://journals.plos.org/plosone/article?id=10.1371/journal.pone.0084646
# Carboplatino
cd=read.csv("cd.csv",header = T)
# Filtered by p-value
cd1=cd[cd$pval <0.05,]
dim(cd1)

#Filtered by fold-change
cd2=cd1[cd1$FC >0.5,]
dim(cd2)
cd3=cd2[cd2$FC >1.5,]
dim(cd3)
```

2. R scripts to model RNA-Seq data under Lotka-Volterra competition equations.

2.1. Cadmium

```
library(ggplot2)

library(deSolve)

# Definir la función de Lotka-Volterra para tres especies
LotkaVolt3 <- function(t, state, parametros) {
  with(as.list(c(state, parametros)), {
    dx1 <- r1 * x1 * (1 - (x1 + a12 * x2) / k1)
    dx2 <- r2 * x2 * (1 - (x2 + a21 * x1) / k2)
    dx3 <- r3 * x3 * (1 - x3 / k3)
    list(c(dx1, dx2, dx3))
  })
}

state3 <- c(x1 = log10(87418.0499439818), x2 = log10(19511.2999667296), x3 =
log10(87418.0499439818))

aa12=round(87418.0499439818/(87418.0499439818+19511.2999667296),1)
aa12
aa21=round(19511.2999667296/(87418.0499439818+19511.2999667296),1)
aa21
parametros3 <- c(r1 = 0.75, r2 = -0.75, r3 = 0.75, a12 = -aa12, a21 = -aa21, k1 = 8.8, k2 = 8.8, k3 =
8.6)

k1 = log10(633571200)
k1
k2 = log10(633571200)
k1
k3 = log10(460771200)
k3
# Estado inicial de las poblaciones
# state3 <- c(x1 = log10(1e10), x2 = log10(8e10), x3 = log10(1e10))
# puedo dejar x1 y x2 iguales y no pasa nada, solo se piensa que parten de ese punto.
# Dejé x3 = log10(324179.5) porque está activado solo el growth,
# porque el WE alimenta al DETOX que no está en tumor normal (x3)

# Secuencia de tiempo
tiempos3 <- seq(0, 10, by = 0.1)

# Ejecutar la simulación
out3 <- ode(func = LotkaVolt3, y = state3, times = tiempos3, parms = parametros3)

# Convertir los resultados en un data frame
out3_df <- as.data.frame(out3)
```

```
names(out3_df) <- c("Time", "Species 1", "Species 2", "Species 3")


plot <- ggplot(out3_df, aes(x = Time)) +
  # Área sombreada entre Species 1 y Species 2
  # geom_ribbon(aes(ymin = `Species 1`, ymax = `Species 3`), fill = "grey80", alpha = 0.5) +
  geom_ribbon(aes(ymin = `Species 1`, ymax = pmin(`Species 1`, `Species 3`)), fill = "grey", alpha =
0.5) +

  #   ymax = pmin(Species 1, Species 2): La función pmin asegura que el valor máximo de sombreado
  # sea el mínimo entre las curvas de Species 1 y Species 2, evitando que el área gris sobrepase
  # la línea de "Detox" (Species 2).

  geom_line(aes(y = `Species 1`, linetype = "Growth"), color = "black", size = 1) +
  geom_line(aes(y = `Species 2`, linetype = "Detox"), color = "black", size = 1, linetype = "dotted") +
  geom_line(aes(y = `Species 3`, linetype = "Growth no pollutant exposure"), color = "black", size = 1,
linetype = "dashed") +

  labs(
    x = "Time",
    y = expression(log[10]~"(ATP molecules)")
  ) +
  scale_linetype_manual(values = c("solid", "dotted", "dashed")) +
  theme_minimal() +
  theme(legend.position = "none") +
  theme(
    legend.title = element_blank(),
    legend.key.width = unit(1.5, "cm"),
    panel.grid.major = element_blank(),  # Eliminar cuadrícula mayor
    panel.grid.minor = element_blank(),  # Eliminar cuadrícula menor
    axis.line = element_line(color = "black"), # Agregar líneas negras a los ejes
    axis.ticks = element_line(color = "black"),
    axis.text.y = element_text(size = 14),
    axis.text.x = element_text(size = 14),
    axis.title.x = element_text(size = 14),
    axis.title.y = element_text(size = 14),
    plot.title = element_text(size = 20, face = "bold")
  )  +
  annotate("text", x = c(6), y = 5, label = "Cd", size = 10)
# +
#   annotate("text", x = c(75), y = 5, label = "DETOX", size = 4) +
#   annotate("text", x = c(35), y = 50, label = "NET", size = 4) +
#   annotate("text", x = c(35), y = 85, label = "ET", size = 4)+
#   annotate("text", x = c(70), y = 85, label = expression(italic(K2)), size = 3)+
#   annotate("text", x = c(70), y = 73, label = expression(italic(K1)), size = 3)

print(plot)
```

2.2 Copper

```
library(ggplot2)

library(deSolve)

# Definir la función de Lotka-Volterra para tres especies
LotkaVolt3 <- function(t, state, parametros) {
  with(as.list(c(state, parametros)), {
    dx1 <- r1 * x1 * (1 - (x1 + a12 * x2) / k1)
    dx2 <- r2 * x2 * (1 - (x2 + a21 * x1) / k2)
    dx3 <- r3 * x3 * (1 - x3 / k3)
    list(c(dx1, dx2, dx3))
  })
}

state3 <- c(x1 = log10(197848.113884089), x2 = log10(59336.863793455), x3 =
log10(197848.113884089))

aa12=round(197848.113884089/(197848.113884089+59336.863793455),1)
aa12
aa21=round(59336.863793455/(197848.113884089+59336.863793455),1)
aa21
parametros3 <- c(r1 = 0.75, r2 = -0.75, r3 = 0.75, a12 = -aa12, a21 = -aa21, k1 = 8.8, k2 = 8.8, k3 =
8.6)
# parametros3 <- c(r1 = 0.75, r2 = -0.75, r3 = 0.75, a12 = -0.5, a21 = -0.5, k1 = 8.8, k2 = 8.8, k3 = 8.6)
k1 = log10(633571200)
k1
k2 = log10(633571200)
k1
k3 = log10(460771200)
k3
# Estado inicial de las poblaciones
# state3 <- c(x1 = log10(1e10), x2 = log10(8e10), x3 = log10(1e10))
state3 <- c(x1 = log10(197848.113884089), x2 = log10(59336.863793455), x3 =
log10(197848.113884089))
# puedo dejar x1 y x2 iguales y no pasa nada, solo se piensa que parten de ese punto.
# Dejé x3 = log10(324179.5) porque está activado solo el growth,
# porque el WE alimenta al DETOX que no está en tumor normal (x3)

# Secuencia de tiempo
tiempos3 <- seq(0, 10, by = 0.1)

# Ejecutar la simulación
out3 <- ode(func = LotkaVolt3, y = state3, times = tiempos3, parms = parametros3)

# Convertir los resultados en un data frame
out3_df <- as.data.frame(out3)
```

```
names(out3_df) <- c("Time", "Species 1", "Species 2", "Species 3")


plot <- ggplot(out3_df, aes(x = Time)) +
  # Área sombreada entre Species 1 y Species 2
  # geom_ribbon(aes(ymin = `Species 1`, ymax = `Species 3`), fill = "grey80", alpha = 0.5) +
  geom_ribbon(aes(ymin = `Species 1`, ymax = pmin(`Species 1`, `Species 3`)), fill = "grey", alpha =
0.5) +

  #   ymax = pmin(Species 1, Species 2): La función pmin asegura que el valor máximo de sombreado
  # sea el mínimo entre las curvas de Species 1 y Species 2, evitando que el área gris sobrepase
  # la línea de "Detox" (Species 2).

  geom_line(aes(y = `Species 1`, linetype = "Growth"), color = "black", size = 1) +
  geom_line(aes(y = `Species 2`, linetype = "Detox"), color = "black", size = 1, linetype = "dotted") +
  geom_line(aes(y = `Species 3`, linetype = "Growth no pollutant exposure"), color = "black", size = 1,
linetype = "dashed") +

  labs(
    x = "Time",
    y = expression(log[10]~"(ATP molecules)")
  ) +
  scale_linetype_manual(values = c("solid", "dotted", "dashed")) +
  theme_minimal() +
  theme(legend.position = "none") +
  theme(
    legend.title = element_blank(),
    legend.key.width = unit(1.5, "cm"),
    panel.grid.major = element_blank(),  # Eliminar cuadrícula mayor
    panel.grid.minor = element_blank(),  # Eliminar cuadrícula menor
    axis.line = element_line(color = "black"), # Agregar líneas negras a los ejes
    axis.ticks = element_line(color = "black"),
    axis.text.y = element_text(size = 14),
    axis.text.x = element_text(size = 14),
    axis.title.x = element_text(size = 14),
    axis.title.y = element_text(size = 14),
    plot.title = element_text(size = 20, face = "bold")
  ) +
  annotate("text", x = c(6), y = 5, label = "Cu", size = 10)
# +
#   annotate("text", x = c(75), y = 5, label = "DETOX", size = 4) +
#   annotate("text", x = c(35), y = 50, label = "NET", size = 4) +
#   annotate("text", x = c(35), y = 85, label = "ET", size = 4)+
#   annotate("text", x = c(70), y = 85, label = expression(italic(K2)), size = 3)+
#   annotate("text", x = c(70), y = 73, label = expression(italic(K1)), size = 3)

print(plot)
```

2.3 Carboplatin

```
library(ggplot2)

library(deSolve)

# Definir la función de Lotka-Volterra para tres especies
LotkaVolt3 <- function(t, state, parametros) {
  with(as.list(c(state, parametros)), {
    dx1 <- r1 * x1 * (1 - (x1 + a12 * x2) / k1)
    dx2 <- r2 * x2 * (1 - (x2 + a21 * x1) / k2)
    dx3 <- r3 * x3 * (1 - x3 / k3)
    list(c(dx1, dx2, dx3))
  })
}

state3 <- c(x1 = log10(5086104.46972098), x2 = log10(543118.082787539), x3 =
log10(5086104.46972098))

aa12=round(5086104.46972098/(5086104.46972098+543118.082787539),1)
aa12
aa21=round(543118.082787539/(5086104.469720989+543118.082787539),1)
aa21
parametros3 <- c(r1 = 0.75, r2 = -0.75, r3 = 0.75, a12 = -aa12, a21 = -aa21, k1 = 8.8, k2 = 8.8, k3 =
8.6)
# parametros3 <- c(r1 = 0.75, r2 = -0.75, r3 = 0.75, a12 = -0.5, a21 = -0.5, k1 = 8.8, k2 = 8.8, k3 = 8.6)
k1 = log10(633571200)
k1
k2 = log10(633571200)
k1
k3 = log10(460771200)
k3
# Estado inicial de las poblaciones
# state3 <- c(x1 = log10(1e10), x2 = log10(8e10), x3 = log10(1e10))
state3 <- c(x1 = log10(197848.113884089), x2 = log10(59336.863793455), x3 =
log10(197848.113884089))
# puedo dejar x1 y x2 iguales y no pasa nada, solo se piensa que parten de ese punto.
# Dejé x3 = log10(324179.5) porque está activado solo el growth,
# porque el WE alimenta al DETOX que no está en tumor normal (x3)

# Secuencia de tiempo
tiempos3 <- seq(0, 10, by = 0.1)

# Ejecutar la simulación
out3 <- ode(func = LotkaVolt3, y = state3, times = tiempos3, parms = parametros3)

# Convertir los resultados en un data frame
```

```
out3_df <- as.data.frame(out3)
names(out3_df) <- c("Time", "Species 1", "Species 2", "Species 3")


plot <- ggplot(out3_df, aes(x = Time)) +
  # Área sombreada entre Species 1 y Species 2
  # geom_ribbon(aes(ymin = `Species 1`, ymax = `Species 3`), fill = "grey80", alpha = 0.5) +
  geom_ribbon(aes(ymin = `Species 1`, ymax = pmin(`Species 1`, `Species 3`)), fill = "grey", alpha =
0.5) +

  #   ymax = pmin(Species 1, Species 2): La función pmin asegura que el valor máximo de sombreado
  # sea el mínimo entre las curvas de Species 1 y Species 2, evitando que el área gris sobrepase
  # la línea de "Detox" (Species 2).

  geom_line(aes(y = `Species 1`, linetype = "Growth"), color = "black", size = 1) +
  geom_line(aes(y = `Species 2`, linetype = "Detox"), color = "black", size = 1, linetype = "dotted") +
  geom_line(aes(y = `Species 3`, linetype = "Growth no pollutant exposure"), color = "black", size = 1,
linetype = "dashed") +

  labs(
    x = "Time",
    y = expression(log[10]~"(ATP molecules)")
  ) +
  scale_linetype_manual(values = c("solid", "dotted", "dashed")) +
  theme_minimal() +
  theme(legend.position = "none") +
  theme(
    legend.title = element_blank(),
    legend.key.width = unit(1.5, "cm"),
    panel.grid.major = element_blank(),  # Eliminar cuadrícula mayor
    panel.grid.minor = element_blank(),  # Eliminar cuadrícula menor
    axis.line = element_line(color = "black"), # Agregar líneas negras a los ejes
    axis.ticks = element_line(color = "black"),
    axis.text.y = element_text(size = 14),
    axis.text.x = element_text(size = 14),
    axis.title.x = element_text(size = 14),
    axis.title.y = element_text(size = 14),
    plot.title = element_text(size = 20, face = "bold")
  ) +
  annotate("text", x = c(6), y = 5, label = "Carboplatin", size = 10)
#
#   annotate("text", x = c(75), y = 5, label = "DETOX", size = 4) +
#   annotate("text", x = c(35), y = 50, label = "NET", size = 4) +
#   annotate("text", x = c(35), y = 85, label = "ET", size = 4)+
#   annotate("text", x = c(70), y = 85, label = expression(italic(K2)), size = 3)+
#   annotate("text", x = c(70), y = 73, label = expression(italic(K1)), size = 3)

print(plot)
```

3. Shell scripting to quantify ATP molecules synthesized in transcript translation

```
#!/bin/bash

# Check if the FASTA file is provided as an argument
if [ "$#" -ne 1 ]; then
    echo "Usage: $0 fasta_file"
    exit 1
fi

# Input FASTA file
fasta_file="$1"

# Dictionary with amino acid values
declare -A valores
valores=(
    [A]=12.5 [R]=18.5 [N]=4 [D]=1 [C]=24.5 [E]=8.5 [Q]=9.5
    [G]=14.5 [H]=33 [I]=20 [L]=33 [K]=18.5 [M]=18.5 [F]=63
    [P]=12.5 [S]=15 [T]=6 [W]=78.5 [Y]=56.5 [V]=25
)

# Process the FASTA file
awk -v vals="${!valores[*]}" -v valores="${valores[*]}" '
BEGIN {
    # Create a dictionary with the values
    split(vals, aa_keys, " ");
    split(valores, aa_vals, " ");
    for (i in aa_keys) {
        amino_values[aa_keys[i]] = aa_vals[i];
    }
}
/^>/ {
    if (sequence != "") {
        # Calculate the weight of the previous sequence
        total_weight = 0;
        for (aa in amino_count) {
            total_weight += amino_count[aa] * amino_values[aa];
        }
        print header ": " total_weight;
        delete amino_count;
    }
    # New sequence, save the header
    header = $0;
    sequence = "";
}
!/^>/ {
    # Count each amino acid in the sequence
    sequence = sequence $0;
```

```
        for (i = 1; i <= length($0); i++) {
            aa = substr($0, i, 1);
            amino_count[aa]++;
        }
    }
    END {
        # Calculate the weight of the last sequence
        total_weight = 0;
        for (aa in amino_count) {
            total_weight += amino_count[aa] * amino_values[aa];
        }
        print header ": " total_weight;
    }
    ' "$fasta_file"
```